Journal of Applied Mathematics and Physics, 2024, 12, 2452-2466
https://www.scirp.org/journal/jamp
ISSN Online: 2327-4379
ISSN Print: 2327-4352

High-Order Soliton Solutions and Hybrid Behavior for the (2 + 1)-Dimensional Konopelchenko-Dubrovsky Equations

Xingying Li, Yin Ji*

College of Mathematics and Statistics, Jishou University, Jishou, China
Email: *1726277751@qq.com

How to cite this paper: Li, X.Y. and Ji, Y. (2024) High-Order Soliton Solutions and Hybrid Behavior for the (2 + 1)-Dimensional Konopelchenko-Dubrovsky Equations. *Journal of Applied Mathematics and Physics*, 12, 2452-2466.
https://doi.org/10.4236/jamp.2024.127147

Received: June 16, 2024
Accepted: July 16, 2024
Published: July 19, 2024

Abstract

In this paper, the evolutionary behavior of *N*-solitons for a (2 + 1)-dimensional Konopelchenko-Dubrovsky equations is studied by using the Hirota bilinear method and the long wave limit method. Based on the *N*-soliton solution, we first study the evolution from *N*-soliton to *T*-order ($T = 1, 2$) breather wave solutions via the paired-complexification of parameters, and then we get the *N*-order rational solutions, *M*-order ($M = 1, 2$) lump solutions, and the hybrid behavior between a variety of different types of solitons combined with the parameter limit technique and the paired-complexification of parameters. Meanwhile, we also provide a large number of three-dimensional figures in order to better show the degeneration of the *N*-soliton and the interaction behavior between different *N*-solitons.

Keywords

Konopelchenko-Dubrovsky Equations, Hirota Bilinear Method, *M*-Order Lump Solutions, High-Order Hybrid Solutions, Interaction Behavior

1. Introduction

As one of the three most attractive research directions in nonlinear science (soliton, chaos and fractal theory), soliton theory plays an important role in various fields of natural science. In recent decades, with the rapid development of computer software, the research results of nonlinear partial differential equations (NPDE) are more and more abundant, especially some new analytical structures and new solving methods emerge in endlessly, such as the Hirota bilinear method [1] [2], the Grammian determinant method [3], the Lie group method [4], the Darboux transformation method [5]-[7], and the backlund transformation

[8] [9], etc. Meanwhile, some new analytical structures of NPDE, such as the breather, lump solution and rogue wave are widely investigated [10]-[14].

In the application field of solitons, the research on the solution of NPDE is no longer limited to the fluid field, and its applications in nonlinear optics, plasmas, condensed matter physics and other fields have also been continuously expanded. Very recently, we found that the analytic structure related to hybrid behavior has been reported in many nonlinear systems, hybrid behavior between lump solution and 1-solitons, hybrid behavior between lump solution and breathers, and hybrid behavior between different solitons.

In this paper, we focus on the *N*-soliton and hybrid behavior of a (2 + 1)-dimensional Konopelchenko-Dubrovsky equations (KD):

$$u_t - u_{xxx} - 6\beta u u_x + \frac{3}{2}\alpha^2 u^2 u_x - 3\left(\int_{-\infty}^{x} u_y \mathrm{d}x\right)_y + 3\alpha u_x \cdot \int_{-\infty}^{x} u_y \mathrm{d}x = 0, \quad (1)$$

where α, β are some arbitrary constants, which reflects richer physical meaning in nonlinear shallow waves.

As a generalized (2 + 1)-dimensional model, the KD equation has received widespread attention from the scientific community since its derivation, and research results have been continuously enriched. KD equation is mainly used in the study of weak dispersion characterization in physics, but also has a wide range of applications in nonlinear optics and plasma physics. Many scholars have contributed to the field of atmospheric science by studying the behavior of nonlinear waves to further reveal subtle scattering effects and large-scale interactions in the troposphere in the tropics and mid-latitudes, and understanding their dynamic behavior is important for understanding weather patterns. In 2001, Lin and Lou gave its multi-soliton solution [15]; Zhi H obtained its traveling wave solution using the hyperbolic tangent function method [16]; Cao obtained the exact multi-parameter solution on the basis of Xu's stability method [17]; by combining the lie symmetry group with the idea of homologous testing, Kang and others gave the non-traveling wave soliton hybrid behavior with arbitrary time function, soliton-like solution and elliptic periodic solitary wave hybrid behavior [18]-[20]. However, to our knowledge, the evolution behavior and interaction phenomenon of some higher-order soliton solutions of KD, including hybrid phenomenon between high-order lump solution and soliton, hybrid behavior between lump solution and *N*-soliton, have not been studied and discussed.

The outline of the paper is as follows: In Section 2, based on the bilinear form of KD Equation (1), we will study the evolution behavior of the *N*-soliton by employing the long wave limit method and the paired-complexification technique of parameters, including the emergence of lump solutions and breather solutions, the hybrid phenomenon of different soliton solutions, interaction of high-order lump solutions. In Section 3, we will study the interaction between the 1-order lump solution and the 1-soliton, 1-order lump solution and the 2-soliton, and the 1-order lump solution and 1-order breather solution. Finally, the conclusion is given in Section 4.

2. Evolution Behavior of *N*-Soliton Solution

In this section, the evolution behavior of the *N*-soliton solutions of the KD equation will be studied by employing the long wave limit technique, such as the emergence of *T*-order breather soliton and *M*-order lump solution. In order to facilitate subsequent discussions, we will initially simplify the above KD equation and make the following transformation:

$$\int_{-\infty}^{x} u_y \mathrm{d}x = v \Leftrightarrow u_y = v_x. \tag{2}$$

Bringing the above changes into (1) yields:

$$u_t - u_{xxx} - 6\beta u u_x - 3v_y + \frac{3}{2}\alpha^2 u^2 u_x + 3\alpha u_x v = 0. \tag{3}$$

Let's make $\alpha = 0$ and do the following transformation:

$$\begin{cases} u = u_0 + \dfrac{2}{\beta}(\ln f)_{xx} \\ v = v_0 + \dfrac{2}{\beta}(\ln f)_{xy}. \end{cases} \tag{4}$$

where *f* is the test function to be selected. Substituting (4) into (3), we get the bilinear of KD equation in the following form:

$$\left(D_x D_t + u_0 D_x^2 - D_x^4 - 3D_y^2\right) f \cdot f = 0, \tag{5}$$

while the bilinear operator $D_{\_}$ represents the Hirota's bilinear differential operator [2].

2.1. The *N*-Soliton Solutions

To obtain the *N*-soliton solution of (4), we apply the usual perturbation method to expand the test function *f* into the following power series:

$$f = 1 + \epsilon f^{(1)} + \epsilon^2 f^{(2)} + \epsilon^3 f^{(3)} + \cdots, \tag{6}$$

where ϵ is the small parameter. Substituting (6) into (4), and to merge similar terms according to the ϵ th power, there are as follows:

$$\begin{cases} \epsilon : P\left(D_x, D_y, D_Z, D_t\right)\left(f^{(1)} \cdot 1 + 1 \cdot f^{(1)}\right) = 0, \\ \epsilon^2 : P\left(D_x, D_y, D_Z, D_t\right)\left(f^{(2)} \cdot 1 + f^{(1)} \cdot f^{(1)} + 1 \cdot f^{(2)}\right) = 0, \\ \epsilon^3 : P\left(D_x, D_y, D_Z, D_t\right)\left(f^{(3)} \cdot 1 + f^{(2)} \cdot f^{(1)} + f^{(1)} \cdot f^{(2)} + 1 \cdot f^{(3)}\right) = 0, \\ \vdots \end{cases} \tag{7}$$

When $N = 1$, take $f^{(1)} = \mathrm{e}^{\eta}, \epsilon = 1$ in (4), according to (4), then there is

$$f = f_1 = 1 + \mathrm{e}^{\eta_1}, f^{(i)} = 0, (i \geq 2), \tag{8}$$

where there is $\eta_1 = k_1\left(m_1 x + p_1 y + q_1 t + r_1\right) + \gamma_1^{(0)}$, and $q_1 = -u_0 m_1 + k_1^2 m_1^3 + 3\dfrac{p_1^2}{m_1}$. Therefore, substituting the above expression into (4) yields the 1-soliton solution.

$$\begin{cases} u(x,y,t) = u_0 + \dfrac{k_1^2 m_1^2}{2\beta}\operatorname{sech}^2\left(\dfrac{1}{2}k_1\left(m_1 x + p_1 y + q_1 t\right) + \dfrac{1}{2}r_1\right), \\ v(x,y,t) = v_0 + \dfrac{k_1^2 m_1 p_1}{2\beta}\operatorname{sech}^2\left(\dfrac{1}{2}k_1\left(m_1 x + p_1 y + q_1 t\right) + \dfrac{1}{2}r_1\right). \end{cases} \tag{9}$$

When $N = 2$, take $f^{(1)} = e^{\eta_1} + e^{\eta_2}, \epsilon = 1$ in (4), we can get

$$\begin{aligned} &f^{(2)} = e^{\eta_1+\eta_2+A_{12}},\ f^{(i)} = 0, (i \geq 3), \\ &F = f_2 = 1 + e^{\eta_1} + e^{\eta_2} + e^{\eta_1+\eta_2+A_{12}}. \end{aligned} \tag{10}$$

The following relationships are established:

$$\begin{cases} \eta_i = k_i\left(m_i x + p_i y + \left(-u_0 m_1 + k_1^2 m_1^3 + 3\dfrac{p_1^2}{m_1}\right)t + r_i\right) + \gamma_i^{(0)}, (i = 1,2), \\ e^{A_{12}} = \dfrac{m_1^2 m_2\left(k_1 m_1 - k_2 m_2\right)^4 - \left(-p_2 m_1 + p_1 m_2\right)^2}{m_1^2 m_2\left(k_1 m_1 + k_2 m_2\right)^4 - \left(-p_2 m_1 + p_1 m_2\right)^2}. \end{cases} \tag{11}$$

Substituting (10) and (11) into (4), we can get the 2-soliton solution,

$$\begin{cases} u(x,y,t) = u_0 + \dfrac{2}{\beta}\ln\left(1 + e^{\eta_1} + e^{\eta_2} + e^{\eta_1+\eta_2+\Lambda_{12}}\right)_{xx}, \\ v(x,y,t) = v_0 + \dfrac{2}{\beta}\ln\left(1 + e^{\eta_1} + e^{\eta_2} + e^{\eta_1+\eta_2+\Lambda_{12}}\right)_{xy}. \end{cases} \tag{12}$$

When $N = 3$, take $f^{(1)} = e^{\eta_1} + e^{\eta_2} + e^{\eta_3}, \epsilon = 1$ in (4), then we can obtain that

$$\begin{aligned} &f^{(2)} = e^{\eta_1+\eta_2+A_{12}} + e^{\eta_1+\eta_3+A_{13}} + e^{\eta_2+\eta_3+A_{23}}, \\ &f^{(3)} = e^{\eta_1+\eta_2+\eta_3+A_{12}+A_{13}+A_{23}},\ f^{(i)} = 0, (i \geq 4), \end{aligned} \tag{13}$$

and

$$\begin{aligned} F = f_3 = 1 &+ e^{\eta_1} + e^{\eta_2} + e^{\eta_3} + e^{\eta_1+\eta_2+A_{12}} + e^{\eta_1+\eta_3+A_{13}} \\ &+ e^{\eta_2+\eta_3+A_{23}} + e^{\eta_1+\eta_2+\eta_3+A_{12}+A_{13}+A_{23}}. \end{aligned} \tag{14}$$

Similarly, substituting the above expression into (4), the 3-soliton solution can be solved.

Based on the Hirota's bilinear Equation (3), the *N*-order soliton solutions of KD Equation (1) can be obtained

$$f = f_N = \sum_{\mu=0,1}\exp\left(\sum_{i=1}^{N}\mu_i\eta_i + \sum_{i<j}^{(N)}A_{ij}\mu_i\mu_j\right), \tag{15}$$

where the $\sum_{\mu=0,1}$ represents summation over all possible combinations of $\mu_1 = 0,1, \mu_2 = 0,1, \cdots, \mu_N = 0,1$, and the $\sum_{i<j}^{(N)}$ is over all possible combinations of the N elements with the specific condition $i < j$. By combining (3) and (4), we get the parameter relationship as

$$\begin{cases} \eta_i = k_i\left(m_i x + p_i y + \left(-u_0 m_1 + k_1^2 m_1^3 + 3\dfrac{p_1^2}{m_1}\right)t + r_i\right) + \gamma_i^{(0)}, \\ \exp\left(A_{ij}\right) = \dfrac{m_i^2 m_j^2\left(k_i m_i - k_j m_j\right)^2 - \left(p_i m_j - p_j m_i\right)^2}{m_i^2 m_j^2\left(k_i m_i + k_j m_j\right)^2 - \left(p_i m_j - p_j m_i\right)^2}. \end{cases} \tag{16}$$

where $p_i \neq 0, m_i \neq 0$ and k_i, p_i, γ_i are some free parameters. Substituting (4) with (5) into (2), we can obtain the N-soliton solutions of KD Equation (1).

In order to better show the evolution behavior of the N-soliton solution with the increase of the soliton number N, we give the spatial structure evolution diagram in Figure 1, with different parameter values as

1): $(u_0, v_0, k_1, m_1, p_1, \gamma_1, \beta, t) = \left(1, \frac{1}{4}, 1, -\frac{1}{5}, 0, 1, 0\right)$,

2): $(u_0, v_0, k_1, k_2, m_1, m_2, p_1, p_2, \gamma_1, \gamma_2, \beta, t) = \left(1, 1, 1, \frac{3}{4}, 1, -1, -2, 2, 3, 2, 1, 0\right)$,

3): $$(u_0, v_0, k_1, k_2, k_3, m_1, m_2, m_3, p_1, p_2, p_3, \gamma_1, \gamma_2, \gamma_3, \beta, t) = \left(2, 2, 1, \frac{3}{2}, 2, 2, 1.1, \frac{1}{2}, \frac{1}{2}, 1, -1, 2, 1, 2, 2, 0\right).$$

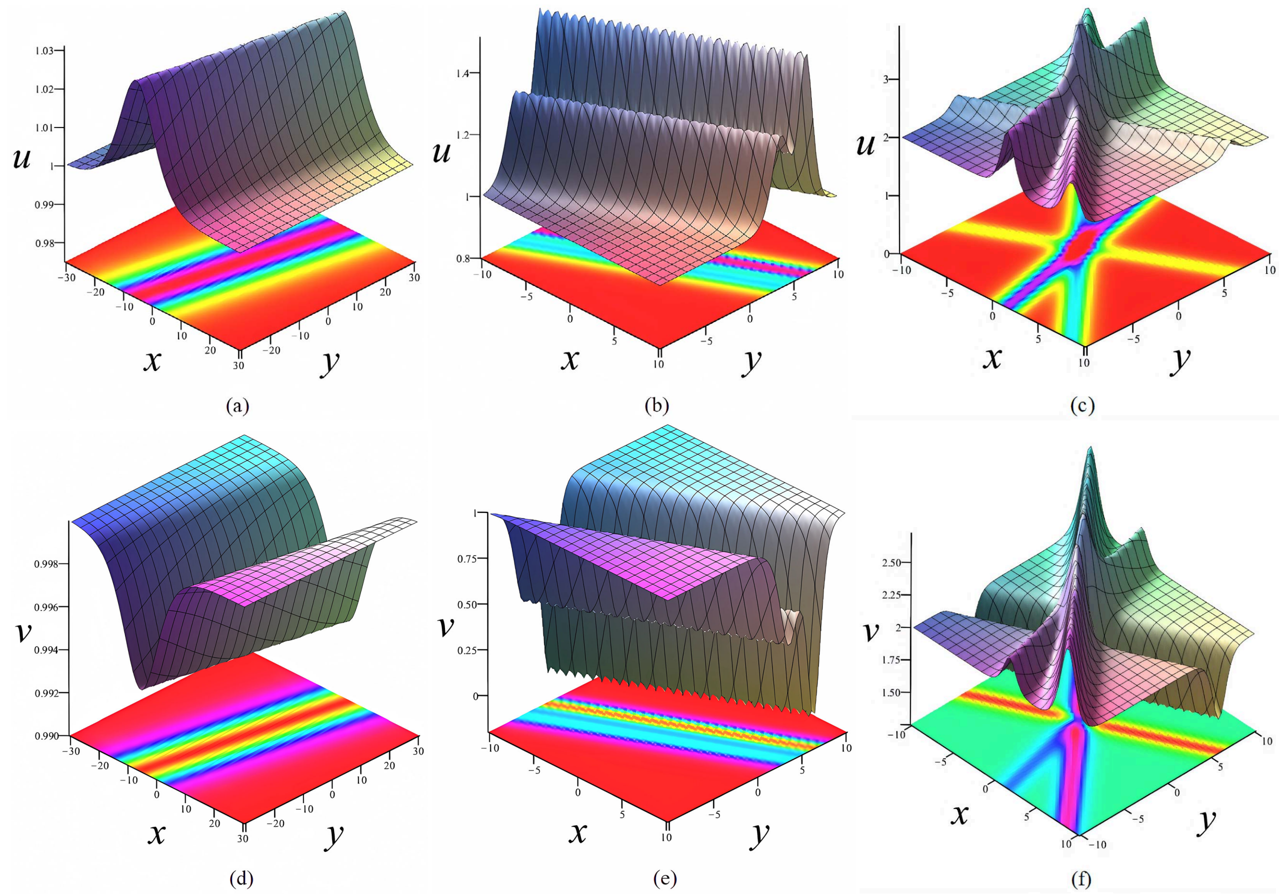

Figure 1. Spatial evolution images of N-soliton solutions u and v at $t = 0$: (a) $N = 1$; (b) $N = 2$; (c) $N = 3$.

2.2. From N-Soliton to T-Order Breather Soliton

The purpose of this section is to construct high-order breather soliton of KD. Since f_N contains free parameters k_i, p_i and γ_i, we cannot get the breather soliton of KD Equation (1) when these parameters take some different values. However, the paired-complexification of parameters k_i, p_i, γ_i can yield smooth breather soliton of KD on a zero background.

Based on the idea of the paired-complexification of parameters, we take the following parameter relations in (17),

$$\begin{aligned}&N=2M,\, m_{M+j}=m_j^*=a_{j1}-a_{j2}I,\, k_{M+j}=k_j^*=b_{j1}-b_{j2}I,\\&p_{M+j}=p_j^*=c_{j1}-c_{j2}I,\, \gamma_{j+1}=\gamma_j^*,\left(j=1,2,\cdots,M\right),\end{aligned} \tag{17}$$

where I means imaginary units. By combining (4), (5), (15) and (17), we can obtain the T-order breather soliton of KD equation.

For example, to construct the 1-order breather soliton, we take $T=2$ in (4), then,

$$f_2=1+\mathrm{e}^{\eta_1}+\mathrm{e}^{\eta_2}+\mathrm{e}^{A_{12}}\mathrm{e}^{\eta_1+\eta_2}. \tag{18}$$

According to (18) and taking $m_2=m_1^*=a_{11}-a_{12}I$, $k_2=k_1^*=b_{11}-b_{12}I$, $p_2=p_1^*=c_{11}-c_{12}I$, $\gamma_2=\gamma_1=\gamma_0$ in (16), we get

$$\tilde{f}_2=2\mathrm{e}^{\varphi_1}\left(\sqrt{M}\cosh\left(\varphi_1+\ln\sqrt{M}\right)+\cos\left(\varphi_2\right)\right),$$

where

$$\begin{aligned}&\varphi_1=a_{11}x+\left(a_{11}b_{11}-a_{12}b_{12}\right)y-\left(a_{11}\omega_{11}-a_{12}\omega_{12}\right)t+\gamma_0,\\&\varphi_2=a_{12}x+\left(a_{11}b_{12}+a_{12}b_{11}\right)y-\left(a_{11}\omega_{12}+a_{12}\omega_{11}\right)t+\gamma_0,\\&M=\mathrm{e}^{A_{12}},\end{aligned} \tag{19}$$

and the parameters $a_{11},a_{12},b_{11},b_{12},\gamma_0$ are some arbitrary real numbers.

Then, the 1-order breather solution can be obtained via inserting $\tilde{f}_2$ into transformation (4),

$$u\left(x,y,t\right)=\frac{2a_{11}\left(\sqrt{M}\cosh\left(\varphi_1+\ln\sqrt{M}\right)+\cos\left(\varphi_2\right)\right)+2a_{11}\sqrt{M}\sinh\left(\varphi_1+\ln\sqrt{M}\right)-2a_{12}\sin\left(\varphi_2\right)}{\sqrt{M}\cosh\left(\varphi_1+\ln\sqrt{M}\right)+\cos\left(\varphi_2\right)}. \tag{20}$$

The 1-order breather solution (20) contains some free parameters, and we can get some 1-order breather solution with different spatial structures by selecting different parameter values.

Similarly, taking $T=4$, we can get the 2-order breather solution of KD Equation (1). In order to better show the evolution behavior of the T-order breather soliton, we give the spatial structure evolution diagram in **Figure 2**, with different parameter values as

1): $$\begin{aligned}&\left(u_0,k_1,k_2,m_1,m_2,p_1,p_2,\gamma_1,\gamma_2,\beta,t\right)\\&=\left(1,1,-1,\frac{1}{2}+I,\frac{1}{2}-I,-2+\frac{1}{2}I,-2-\frac{1}{2}I,0,0,\frac{1}{2},0\right),\end{aligned}$$

2): $$\begin{aligned}&\left(u_0,v_0,k_1,k_2,m_1,m_2,p_1,p_2,\gamma_1,\gamma_2,\beta,t\right)\\&=\left(1,1,1,1,1+2I,1-2I,-\frac{1}{2}+I,-\frac{1}{2}-I,0,0,2,0\right),\end{aligned}$$

3): $$\begin{aligned}&\left(u_0,k_1,k_2,k_3,k_4,m_1,m_2,m_3,m_4,p_1,p_2,p_3,p_4,\gamma_1,\gamma_2,\gamma_3,\gamma_4,\beta,t\right)\\&=\left(0,1,1,1,1,-1+1I,-1-1I,2+2I,2-2I,2+2I,2-2I,1+2I,1-2I,0,0,0,0,\frac{1}{2},0\right),\end{aligned}$$

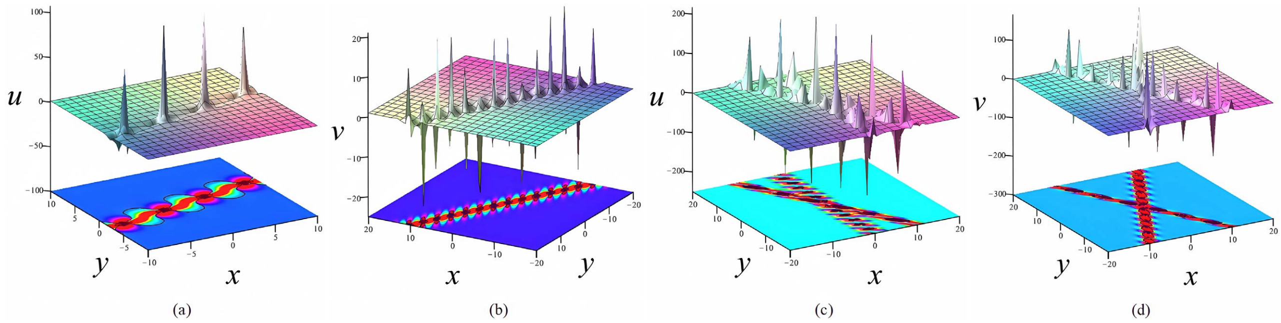

Figure 2. Spatial evolution images of T-breather solutions u and v at $t=0$: (a) and (b): $T=1$; (c) and (d): $T=2$.

4):

$$\left(v_0,k_1,k_2,k_3,k_4,m_1,m_2,m_3,m_4,p_1,p_2,p_3,p_4,\gamma_1,\gamma_2,\gamma_3,\gamma_4,\beta,t\right)$$
$$=\left(0,2,2,2,2,-1+1I,-1-1I,2+I,2-I,\frac{1}{2}+\frac{1}{2}I,\frac{1}{2}-\frac{1}{2}I,1+I,1-I,0,0,0,0,\frac{1}{2},0\right).$$

By further analysis, we can see that the position of the 1-order breather solution on the (x,y) plane is determined by a_{11} and $a_{11}b_{11}-a_{12}b_{12}$. When $a_{11}=0$ and $a_{11}b_{11}-a_{12}b_{12}\neq 0$, 1-order breather solution is perpendicular to the Y-axis; when $a_{11}\neq 0$ and $a_{11}b_{11}-a_{12}b_{12}=0$, 1-order breather solution is parallel to the Y-axis; when $a_{11}\left(a_{11}b_{11}-a_{12}b_{12}\right)\neq 0$, the slope of 1-order breather solution in the (x,y) plane is $\frac{-a_{11}}{a_{11}b_{11}-a_{12}b_{12}}$. Similar to 1-order breather solution, the position of 2-order breather solution on the plane (x,y) is determined by a_{11}, a_{12}, $a_{11}b_{12}+a_{12}b_{11}$ and $a_{11}b_{11}-a_{12}b_{12}$. When $a_{11}=a_{12}=0$, 2-order breather solution is perpendicular to the Y-axis; when $a_{11}\left(a_{11}b_{11}-a_{12}b_{12}\right)=a_{12}\left(a_{11}b_{12}+a_{12}b_{11}\right)=0$ and $a_{11}\left(a_{11}b_{12}+a_{12}b_{11}\right)\neq a_{12}\left(a_{11}b_{11}-a_{12}b_{12}\right)$, 2-order breather solution is parallel to the Y-axis; when $a_{11}\left(a_{11}b_{11}-a_{12}b_{12}\right)\neq a_{12}\left(a_{11}b_{12}+a_{12}b_{11}\right)$, the cross structure of the solution of 2-order breather in the (x,y) plane can be obtained.

2.3. From *N*-Soliton to *M*-Order Lump Solution

According to the long wave limit technique, we take $k_i/k_j=O(1)$ and let k_i tend to 0 in (21) and (4). Therefore, we get

$$f_N=\sum_{\mu=0,1}\prod_{i=1}^{N}(-1)^{\mu_i}\left(1+\mu_i k_i\theta_i\right)\prod_{i<j}^{(N)}\exp\left(1+\mu_i\mu_j k_i k_j B_{ij}\right)+O\left(k^{N+1}\right), \tag{21}$$

with

$$\begin{cases}\theta_i=m_i x+p_i y+\left(-u_0 m_1+\dfrac{3p_1^2}{m_1}\right)t,\\ \exp\left(A_{ij}\right)\approx 1-\dfrac{4k_i k_j m_i^3 m_j^3}{m_i^2 m_j^2\left(k_i m_i+k_j m_j\right)^4-\left(p_i m_j-p_j m_i\right)^2}\overset{\text{def}}{=}1+k_i k_j B_{ij},\\ B_{ij}=-\dfrac{4m_1^3 m_2^3}{m_1^2 m_2^2\left(k_1 m_1+k_2 m_2\right)^4-\left(p_1 m_2-p_2 m_1\right)^2}.\end{cases} \tag{22}$$

Since u and v is given by transformation (2), we have therefore deduced the following rational solutions,

$$f_N=\prod_{i=1}^{N}\theta_i+\frac{1}{2}\sum_{i,j}^{(N)}B_{ij}\prod_{r\neq i,j}^{N}\theta_r++\frac{1}{2!2^2}\sum_{i,j,p,s}^{(N)}B_{ij}B_{ps}\prod_{r\neq i,j,p,s}^{N}\theta_r+\cdots$$
$$+\frac{1}{M!2^M}\sum_{i,j,\cdots,m,n}^{(N)}\overbrace{B_{ij}B_{kl}\cdots B_{mn}}^{M}\prod_{s\neq i,j,k,l,\cdots,m,n}^{N}\theta_s+\cdots, \tag{23}$$

where $\sum_{i,j,\cdots,m,n}^{(N)}$ denotes the summation over all possible combinations of $i,j,\cdots,m,n$, which are taken different values from these numbers $1,2,\cdots,N$. Choosing $N=1,2,\cdots$ in (24), and substituting it into (2), we can get the N-order rational solution of KD Equation (1).

To obtain M-order lump solution for KD Equation (1), select $N=2M$ and $m_{M+i}=m_i^*=a_i-b_iI$, $p_{M+i}=p_i^*=c_i-d_iI$, $n_{M+i}=n_i^*=e_i-f_iI$, $r_i=0$ $(i=1,2,\cdots,M)$ in Equations (1) and (2), where I represents the imaginary unit and $*$ indicates that the complex number is conjugated taking.

For example, when $N=2$, take $m_2=m_1^*=a_1-b_1I$, $p_2=p_1^*=c_1-d_1I$ in F_2, By simple calculations, we can obtain

$$F_2=\theta_1\theta_2+B_{12}, \tag{24}$$

where

$$\begin{vmatrix}a_1 & b_1\\ c_1 & d_1\end{vmatrix}\neq 0, b_1\neq 0. \tag{25}$$

Substituting (15) into (3) gives the 1-order lump solution solution of the Equation (1) (see Figure 3(a) and Figure 3(b)):

$$\begin{cases}u(x,y,t)=u_0+4\dfrac{\left(a_1^2-b_1^2\right)\left(\xi_1^2-\zeta_1^2\right)+\left(a_1^2+b_1^2\right)\Delta-4a_1b_1\xi_1\zeta_1}{\beta\left(\xi_1^2+\zeta_1^2+\Delta\right)^2},\\ v(x,y,t)=v_0+\dfrac{\left(b_1d_1-a_1c_1\right)\left(\xi_1^2-\xi_1^2\right)+\left(a_1c_1+b_1d_1\right)\Delta-2\left(a_1d_1+b_1c_1\right)\xi_1\zeta_1}{\beta\left(\xi_1^2+\xi_1^2+\Delta\right)^2}.\end{cases} \tag{26}$$

When $N=3,4$, we have

$$\begin{aligned}&f_3=\theta_1\theta_2\theta_3+B_{12}\theta_3+B_{23}\theta_1+B_{31}\theta_2,\\&f_4=\theta_1\theta_2\theta_3\theta_4+B_{12}\theta_3\theta_4+B_{13}\theta_2\theta_4+B_{14}\theta_2\theta_3+B_{23}\theta_1\theta_4+B_{24}\theta_1\theta_3\\&\qquad+B_{34}\theta_1\theta_2+B_{12}B_{34}+B_{13}B_{24}+B_{14}B_{23}.\end{aligned} \tag{27}$$

Similar to the calculation of $N=2$, when $N=4$, $M=2$, taking $p_3=p_1^*=a_1-b_1I$, $p_4=p_2^*=a_2-b_2I$, in (24), we can get 2-order lump solution (see Figure 3(c) and Figure 3(d)). The values of related parameters in Figure 3 are shown as follows:

1): $u_0=0,a_1=\frac{1}{2},b_1=\frac{2}{5},c_1=-1,d_1=\frac{12}{5},\beta=1,t=0$;

2): $v_0=0,a_1=\frac{1}{2},b_1=\frac{1}{5},c_1=\frac{1}{2},d_1=2,\beta=1,t=0$;

3) and 4):

$u_0=2,v_0=2,a_1=\frac{1}{2},b_1=\frac{1}{2},a_2=\frac{1}{2},b_2=\frac{1}{2},c_1=0,d_1=\frac{1}{2},c_2=0,d_2=-\frac{1}{2},\beta=1,t=0$.

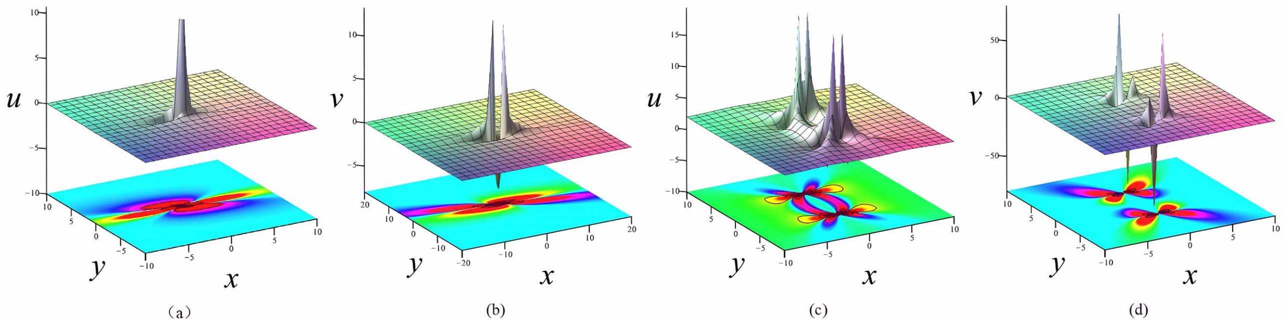

Figure 3. Spatial evolution images of M-order lump solutions u and v at $t = 0$: (a) and (b) $M = 1$; (c) and (d) $M = 2$.

Moreover, when $N = 2M$, taking $p_{M+i} = p_i^* = a_i - b_i I\left(i = 1, 2, \cdots, M\right)$ in (24), we can obtain the M-order lump solution of the KD equation.

In fact, we can note that when $\left(a_{11}, b_{11}\right) \to \left(0, 0\right)$, the period of the 1-order breather solution approaches infinity, and the smooth breather solution is transformed into the 1-order lump solution. Conversely, higher order lump solutions can also be derived from higher order breather solutions.

3. From *N*-Soliton to *L*-Order Hybrid Solution

In this section, we mainly study the high-order hybrid solution of KD (1) by combining the long wave limit technique and the paired-complexification of parameters, including the hybrid solution between the 1-order lump solution and 1-soliton solution, the hybrid solution between the 1-order lump solution and 2-soliton solution, the hybrid solution between the 1-order lump solution and 1-order breather solution.

3.1. A Hybrid Solution between the 1-Order Lump Solution and 1-Soliton

In order to construct the hybrid solution consisting of 1-order lump solution and 1-soliton solution, taking $N = 3$, $\gamma_1 = \gamma_2 = I\pi$ in (4) and f_3 can be written as follows:

$$\begin{aligned} F = f_3 &= 1 + e^{\eta_1} + e^{\eta_2} + e^{\eta_1 + \eta_2 + A_{12}} + e^{\eta_3}\left(1 + e^{\eta_1 + A_{13}} + e^{\eta_2 + A_{23}} + e^{\eta_1 + \eta_2 + A_{12} + A_{13} + A_{23}}\right) \\ &= 1 + e^{k_1\theta_1 + \gamma_1^{(0)}} + e^{k_2\theta_2 + \gamma_2^{(0)}} + e^{k_1\theta_1 + k_2\theta_2 + \gamma_1^{(0)} + \gamma_2^{(0)} + A_{12}} \\ &\quad + e^{\eta_3}\left(1 + e^{k_1\theta_1 + \gamma_1^{(0)}} + e^{k_2\theta_2 + \gamma_2^{(0)}} + e^{k_1\theta_1 + k_2\theta_2 + \gamma_1^{(0)} + \gamma_2^{(0)} + A_{12} + A_{13} + A_{23}}\right), \end{aligned} \tag{28}$$

where

$$\begin{aligned} \eta_i &= k_i\left(m_i x + p_i y + \left(-u_0 m_1 + k_1^2 m_1^3 + 3\frac{p_1^2}{m_1}\right)t + r_i\right) + \gamma_i^{(0)} \\ &\triangleq k_i\theta_i + \gamma_i^{(0)}, \left(i = 1, 2\right). \end{aligned} \tag{29}$$

By combining $e^{\gamma_i^{(0)}} = -1, \left(i = 1, 2\right)$ and simplifying, we can obtain

$$\begin{aligned} F = f_3 &= 1 - e^{k_1\theta_1} - e^{k_2\theta_2} + e^{k_1\theta_1 + k_2\theta_2 + A_{12}} \\ &\quad + e^{\eta_3}\left(1 - e^{k_1\theta_1 + A_{13}} - e^{k_2\theta_2 + A_{23}} + e^{k_1\theta_1 + k_2\theta_2 + A_{12} + A_{13} + A_{23}}\right), \end{aligned} \tag{30}$$

letting $k_1 \to 0, k_2 \to 0$, we get

$$\begin{cases} \theta_i = m_i x + p_i y + \left(-u_0 m_1 + \dfrac{3p_1^2}{m_1}\right)t, \\ \exp(A_{12}) \to 1 + \dfrac{-4k_1k_2m_1^3m_2^3}{m_1^2m_2^2(k_1m_1+k_2m_2)^4 - (p_1m_2 - p_2m_1)^2} \overset{\text{def}}{=} 1 + k_1k_2B_{12}, \\ \exp(A_{13}) \to 1 + \dfrac{-4k_1k_3m_1^3m_3^3}{m_1^2m_3^2(k_1m_1+k_3m_3)^4 - (p_1m_3 - p_3m_1)^2} \overset{\text{def}}{=} 1 + k_1C_{13}, \\ \exp(A_{23}) \to 1 + \dfrac{-4k_2k_3m_2^3m_3^3}{m_2^2m_3^2(k_2m_2+k_3m_3)^4 - (p_2m_3 - p_3m_2)^2} \overset{\text{def}}{=} 1 + k_2C_{23}, \end{cases} \tag{31}$$

and

$$\tilde{f}_3 = \theta_1\theta_2 + B_{12} + (C_{13}C_{23} + C_{13}\theta_2 + C_{23}\theta_1 + \theta_1\theta_2 + B_{12})e^{\eta_3}. \tag{32}$$

Taking $m_2 = m_1^* = a_1 - b_1 I, p_2 = p_1^* = c_1 - d_1 I$ in (31) and (32), and substituting it into (2), we get a hybrid solution between the 1-order lump solution and the 1-soliton (see **Figure 4**). In **Figure 4**, we give the spatial structure evolution diagram of the hybrid solution with time *t*, where the values of the parameters are

$$u: a_1 = \frac{1}{2}, b_1 = 2, c_1 = -2, d_1 = 1, a_2 = \frac{2}{5}, c_2 = \frac{4}{5}, u_0 = 0, v_0 = 0,$$
$$\beta = 1, k_1 = 0, k_2 = 0, k_3 = -\frac{7}{10}, \gamma_3 = 0;$$

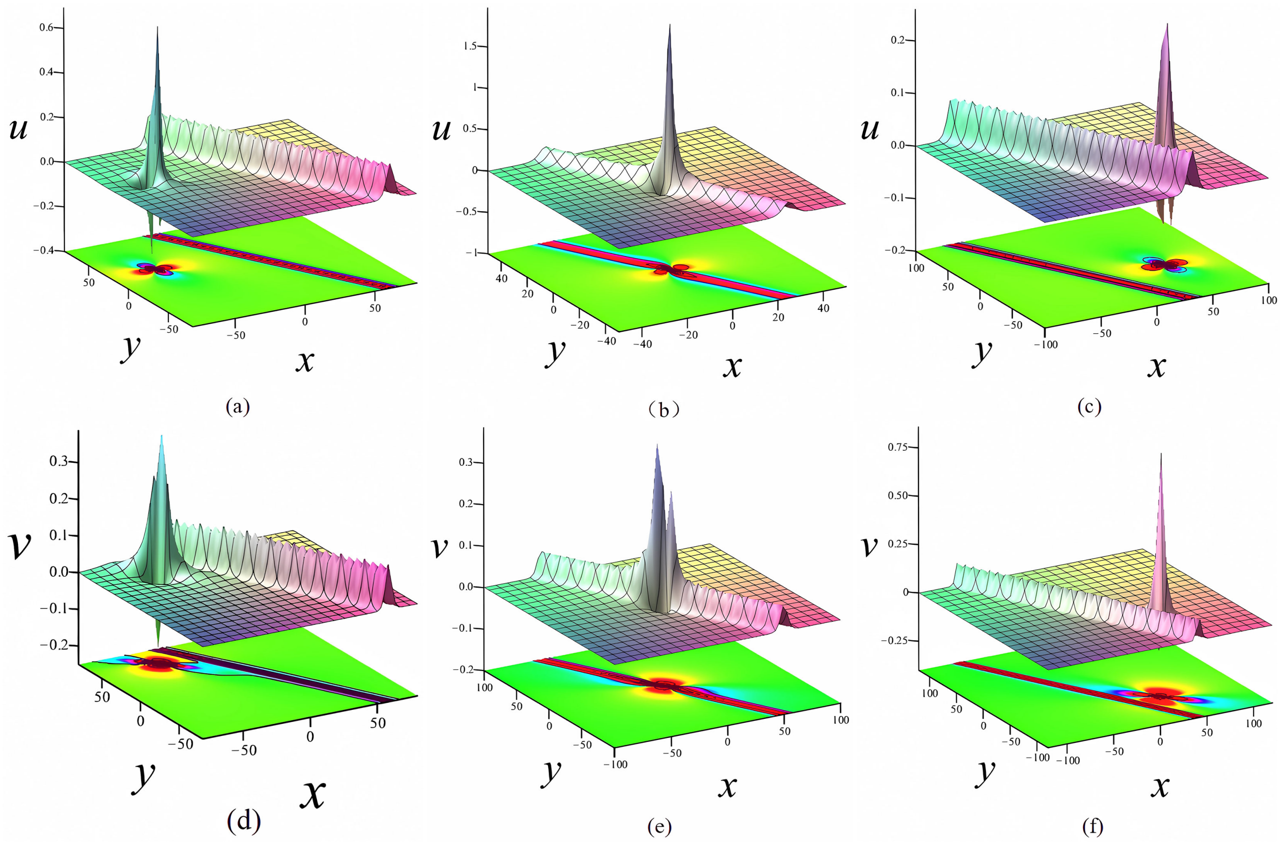

Figure 4. Evolution structure diagram of the hybrid solutions u and v between 1-order lump solution and 1-soliton at different times: (a) $t = -20$; (b) $t = 0$; (c) $t = 20$; (d) $t = -15$; (e) $t = 0$; (f) $t = 15$.

$$v: a_1=-\frac{1}{2}, b_1=2, c_1=-2, d_1=1, a_2=\frac{1}{2}, c_2=1, u_0=0, v_0=0,$$
$$\beta=1, k_1=0, k_2=0, k_3=-\frac{7}{10}, \gamma_3=0.$$

From **Figure 4**, we find that the lump solution and 1-soliton solution do not affect each other's motion during the interaction process, such as the motion speed and amplitude of the lump solution, the shape of the soliton solution, etc. This phenomenon is also known as the complete elastic collision [21].

3.2. A Hybrid Solution between the 1-Order Lump Solution and 2-Soliton

To obtain the hybrid solution consisting of 1-order lump solution and 2-soliton solution, taking $N=4$, $\gamma_1=\gamma_2=I\pi$ in (4) and letting $k_1\to 0, k_2\to 0$, we have

$$\begin{aligned}\tilde{f}_4 &= \theta_1\theta_2+B_{12}+\left(C_{13}C_{23}+C_{13}\theta_2+C_{23}\theta_1+\theta_1\theta_2+B_{12}\right)e^{\eta_3}\\ &+\left(C_{14}C_{24}+C_{14}\theta_2+C_{24}\theta_1+\theta_1\theta_2+B_{12}\right)e^{\eta_4}\\ &+\left(\theta_1\theta_2+\left(C_{23}+C_{24}\right)\theta_1+\left(C_{13}+C_{14}\right)\theta_2+B_{12}+C_{13}C_{23}\right.\\ &\left.+C_{14}C_{23}+C_{13}C_{24}+C_{14}C_{24}\right)e^{\eta_3+\eta_4}\exp\left(A_{34}\right),\end{aligned} \tag{33}$$

where $\theta_i\left(i=1,2\right)$, η_3, B_{12}, $C_{ij}\left(i=1,2; j=3\right)$ are given by (29), the $\exp\left(A_{34}\right)$ is determined by (5), and

$$\begin{aligned}&\eta_4=k_4\left(m_4x+p_4y+\left(-u_0m_1+k_1^2m_1^3+3\frac{p_1^2}{m_1}\right)t+r_4\right)+\gamma_4^{(0)}, p_2=p_1^*=a_1-b_1I,\\ &C_{ij}=\frac{-4k_jm_i^3m_j^3}{m_i^2m_j^2\left(k_im_i+k_jm_j\right)^4-\left(p_im_j-p_jm_i\right)^2}\left(i=1,2; j=4\right).\end{aligned} \tag{34}$$

Then, substituting (33) and (34) into (2), we get a hybrid solution between the 1-order lump solution and the 2-soliton (see **Figure 5**). In **Figure 5**, we give the spatial structure evolution diagram of the hybrid solution with time *t*, where the values of the parameters are

$$u: a_1=-2, b_1=1, a_2=-1, a_3=1, c_1=1, d_1=\frac{3}{2}, c_2=2, c_3=2,$$
$$u_0=0, v_0=0, \beta=2, k_3=\frac{1}{4}, k_4=\frac{1}{4}, \gamma_3=0, \gamma_4=0;$$
$$v: a_1=-2, b_1=1, a_2=-1, a_3=1, c_1=1, d_1=\frac{3}{2}, c_2=2, c_3=2,$$
$$u_0=0, v_0=0, \beta=2, k_3=\frac{2}{5}, k_4=\frac{2}{5}, \gamma_3=0, \gamma_4=0.$$

3.3. A Hybrid Solution between the 1-Order Lump Solution and 1-Order Breather Solution

Unlike the previous hybrid solution of 1-order lump and 2-soliton, here we make the following transformation to obtain a new hybrid solution between the 1-order lump solution and 1-order breather solution:

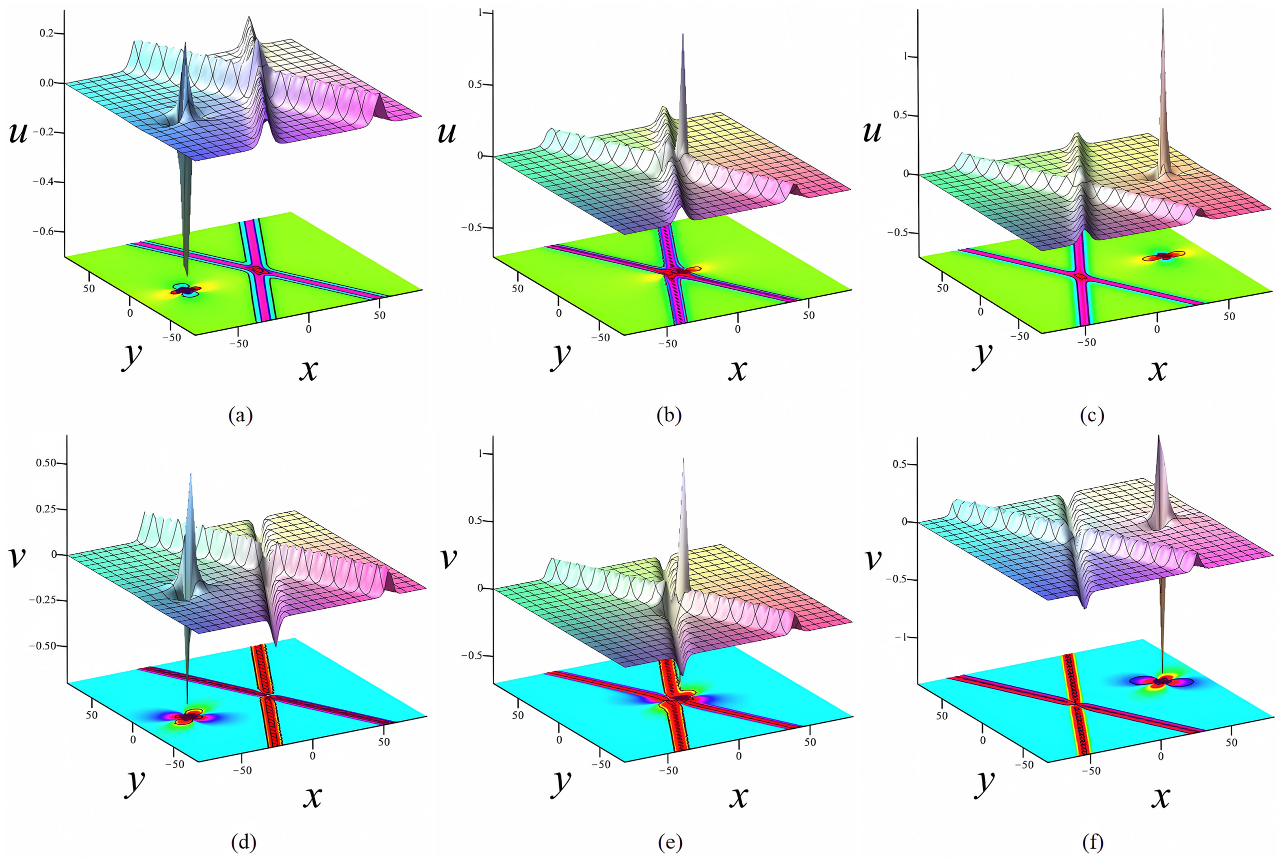

Figure 5. Evolution structure diagram of the hybrid solutions u and v between 1-order lump solution and 2-soliton at different times: (a) $t=-10$; (b) $t=0$; (c) $t=10$; (d) $t=-10$; (e) $t=0$; (f) $t=10$.

$$p_2 = p_1^* = a_1 - b_1 I, p_4 = p_3^* = a_2 - b_2 I, m_2 = m_1^* = c_1 - d_1 I, m_4 = m_3^* = c_2 - d_2 I. \quad (35)$$

We substitute B_{ij} in (22) and C_{ij} in (34), combined with (35), into the following equation:

$$\begin{aligned} f = &\mathrm{e}^{A_{34}}\left(C_{13}C_{23} + C_{14}C_{23} + C_{13}C_{24} + C_{14}C_{24} + C_{13}\theta_2 + C_{14}\theta_2 + C_{23}\theta_1 \right. \\ &\left. + C_{24}\theta_1 + \theta_1\theta_2 + B_{12}\right)\mathrm{e}^{\eta_3+\eta_4} + \left(C_{13}C_{23} + C_{13}\theta_2 + C_{23}\theta_1 + \theta_1\theta_2 + B_{12}\right)\mathrm{e}^{\eta_3} \\ &+ \left(C_{14}C_{24} + C_{14}\theta_2 + C_{24}\theta_1 + \theta_1\theta_2 + B_{12}\right)\mathrm{e}^{\eta_4} + \theta_1\theta_2 + B_{12}. \end{aligned} \quad (36)$$

Next, in the same situation as before, we substitute (36) into (4) and take the relevant parameters to obtain the hybrid solution between the 1-order lump solution and 1-order breather solution. In order to better demonstrate its spatial structure, we provide a demonstration diagram in **Figure 6**, with the relevant parameters as follows:

$$a_1 = -2, b_1 = 2, a_2 = -2, b_2 = 1, c_1 = 1, d_1 = 2, c_2 = 2, d_2 = -2,$$
$$u_0 = 0, v_0 = 0, \beta = 2, k_3 = \frac{1}{5}, k_4 = \frac{1}{5}, \gamma_3 = 0, \gamma_4 = 0.$$

From **Figure 6**, we can see that over time, the lump solution and breather solution interact with each other, and their shapes remain unchanged before and after each other, which indicates that this is an elastic collision.

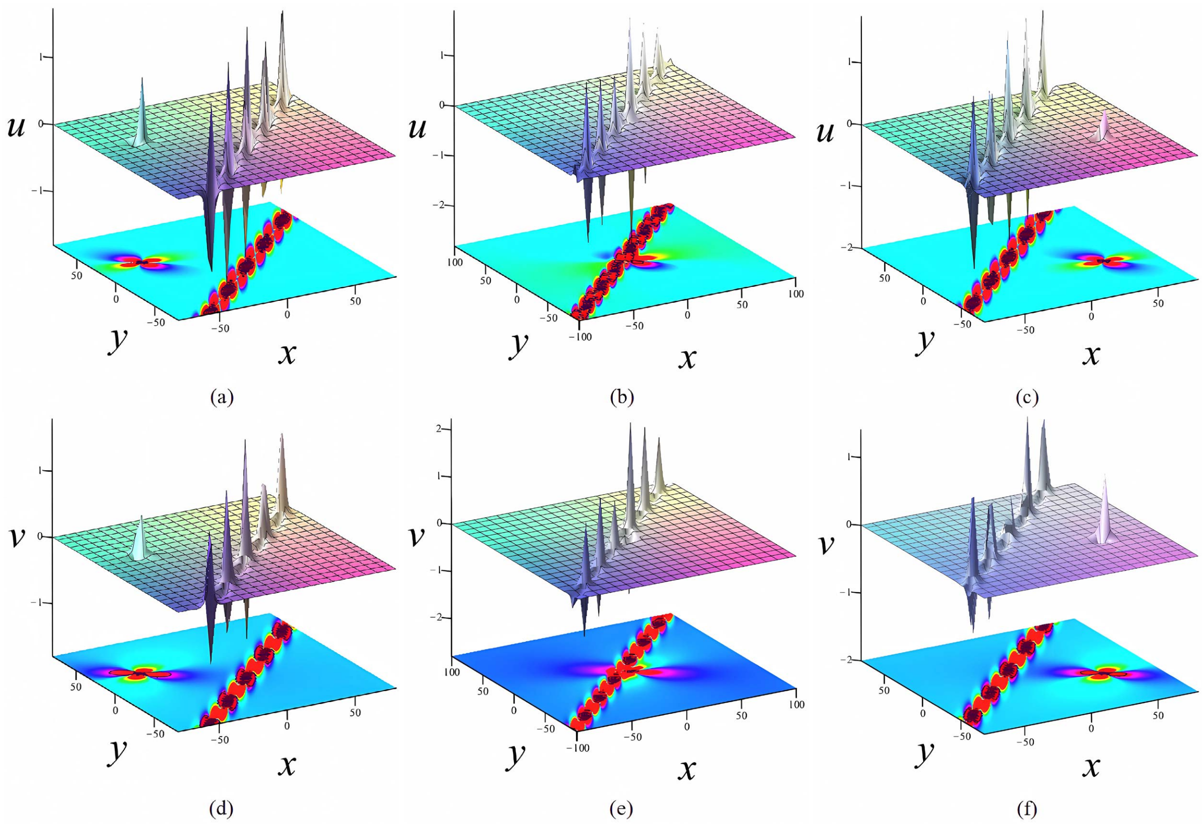

Figure 6. Evolution structure diagram of the hybrid solutions u and v between 1-order lump solution and 1-order breather solution at different times: (a) $t=-10$; (b) $t=0$; (c) $t=10$; (d) $t=-10$; (e) $t=0$; (f) $t=10$.

4. Conclusion

This article is mainly divided into two parts. One part is to use the long wave limit method to obtain a series of solutions to the KD equation. Starting from the N-soliton solution of the KD equation, the first step is to perform parameter complexation to obtain the breather solution of the KD equation. Then, by limiting the parameter k_i, the lump solution of the KD equation is obtained; the other part is based on the series of solutions, selecting different test functions to obtain hybrid solutions of the KD equation, such as the 1-order lump with 1-soliton, 2-soliton and 1-order breather solution. By analyzing the spatial evolution diagram of the hybrid solutions, we found that the three types of hybrid solutions mentioned above are all elastic collisions, and before and after the interaction, the velocity and shape of the waves do not change. The KD equation is a relatively classic class of nonlinear equations, and this article analyzes its different types of solutions, hoping to provide valuable information for the study of mathematical physics.

Acknowledgements

This work was partially supported by the Natural Science Foundation of Hunan Province (No. 2021JJ40434), and the Scientific Research Project of the Hunan Education Department (No. 21B0510).

Conflicts of Interest

The authors declare no conflicts of interest regarding the publication of this paper.

References

[1] Hirota, R. and Satsuma, J. (1981) Soliton Solutions of a Coupled KdV Equation. *Physics Letters A*, **85**, 407-408. https://doi.org/10.1016/0375-9601(81)90423-0

[2] Hirota, R. (2004) The Direct Method in Soliton Theory. Cambridge University Press. https://doi.org/10.1017/CBO9780511543043

[3] Satsuma, J. (1979) A Wronskian Representation of N-Soliton Solutions of Nonlinear Evolution Equations. *Journal of the Physical Society of Japan*, **46**, 359-360. https://doi.org/10.1143/JPSJ.46.359

[4] Olver, P.J. (1986) Application of Lie Groups to Differential Equations. Springer. https://doi.org/10.1007/978-1-4684-0274-2

[5] Wang, M., Tian, B. and Zhou, T.Y. (2021) Darboux Transformation, Generalized Darboux Transformation and Vector Breathers for a Matrix Lakshmanan-Porsezian-Daniel Equation in a Heisenberg Ferromagnetic Spin Chain. *Chaos*, *Solitons and Fractals*, **152**, Article 111411. https://doi.org/10.1016/j.chaos.2021.111411

[6] Jia, T.T., Gao, Y.T., Yu, X., *et al.* (2021) Lax Pairs, Infinite Conservation Laws, Darboux Transformation, Bilinear Forms and Solitonic Interactions for a Combined Calogero-Bogoyavlenskii-Schiff-Type Equation. *Applied Mathematics Letters*, **114**, Article 106702. https://doi.org/10.1016/j.aml.2020.106702

[7] Ling, A., Li, C. and Zhang, L. (2021) Darboux Transformations and Solutions of Nonlocal Hirota and Maxwell-Bloch Equations. *Studies in Applied Mathematics*, **147**, 60-83. https://doi.org/10.1111/sapm.12378

[8] Yan, Z.Y. (2003) Painlevé analysis, auto-Bäcklund transformations and exact solutions for a simplified model for reacting mixtures. *Physica A*: *Statistical Mechanics and Its Applications*, **326**, 344-359. https://doi.org/10.1016/S0378-4371(03)00361-3

[9] Yin, Y.-H., Lü, X. and Ma, W.X. (2022) Bäcklund Transformation, Exact Solutions and Diverse Interaction Phenomena to a (3 + 1)-Dimensional Nonlinear Evolution Equation. *Nonlinear Dynamics*, **108**, 4181-4194. https://doi.org/10.1007/s11071-021-06531-y

[10] Cheng, W.G. and Xu, T.Z. (2018) Lump Solutions and Interaction Behaviors to the (2 + 1)-Dimensional Extended Shallow Water Wave Equation. *Modern Physics Letters B*, **32**, Article 1850387. https://doi.org/10.1142/S0217984918503876

[11] Wang, M., Tian, B., Sun, Y. and Zhang, Z. (2020) Lump, Mixed Lump-Stripe and Rogue Wave-Stripe Solutions of a (3 + 1)-Dimensional Nonlinear Wave Equation for a Liquid with Gas Bubbles. *Computers and Mathematics with Applications*, **79**, 576-587. https://doi.org/10.1016/j.camwa.2019.07.006

[12] Peng, W.Q., Tian, S.F. and Zhang, T.T. (2019) Breather Waves and Rational Solutions in the (3 + 1)-Dimensional Boiti Boiti-Leon-Manna-Pempinelli Equation. *Computers and Mathematics with Applications*, **77**, 715-723. https://doi.org/10.1016/j.camwa.2018.10.008

[13] Yin, H.M., Tian, B. and Zhao, X.C. (2020) Chaotic Breathers and Breather Fission/Fusion for a Vector Nonlinear Schrödinger Equation in a Birefringent Optical Fiber or Wavelength Division Multiplexed System. *Applied Mathematics and Computation*, **368**, Article 124768. https://doi.org/10.1016/j.amc.2019.124768

[14] Tan, W., Zhang, W. and Zhang, J. (2019) Evolutionary Behavior of Breathers and

Interaction Solutions with M-Solitons for (2 + 1)-Dimensional KdV System. *Applied Mathematics Letters*, **101**, Article 106063. https://doi.org/10.1016/j.aml.2019.106063

[15] Lin, J., Lou, S. and Wang, K. (2001) Multi-Soliton Solutions of the Konopelchenko-Dubrovsky Equation. *Chinese Physics Letters*, **18**, Article 1173. https://doi.org/10.1088/0256-307X/18/9/306

[16] Zhi, H. (2008) Lie Point Symmetry and Some New Soliton Like Solutions of the KD Equations. *Applied Mathematics and Computation*, **203**, 931-936. https://doi.org/10.1016/j.amc.2008.05.090

[17] Cao, B.T. (2010) Solutions of Jimbo-Miwa Equation and Konopelchenko-Dubrovsky Equations. *Acta Applicandae Mathematicae*, **112**, 181-203. https://doi.org/10.1007/s10440-009-9559-5

[18] Kang, X.R., Xian, D.Q. and Dai, Z.D. (2016) Symmetry Reductions and Rational Non-Traveling Wave Solutions for the (2 + 1)-D Ablowitz-Kaup-Newell-Segur Equation. *International Journal of Numerical Methods for Heat and Fluid Flow*, **26**, 2331-2339. https://doi.org/10.1108/HFF-05-2015-0204

[19] Zhang, S. (2007) Symbolic Computation and New Families of Exact Non-Travelling Wave Solutions of (2 + 1)-D KD Equation. *Chaos, Solitons and Fractals*, **45**, Article 985. https://doi.org/10.1016/j.chaos.2007.07.062

[20] Song, L. and Zhang, H. (2007) New Exact Solutions for the KD Equation Using Extended Ricati Equation Expansion Method and Symbolic Computation. *Applied Mathematics and Computation*, **187**, 1373-1388. https://doi.org/10.1016/j.amc.2006.09.046

[21] Tan, W., Dai, Z.D., Xie, J.L. and Qiu, D.Q. (2018) Parameter Limit Method and Its Application in the (4 + 1)-Dimensional Fokas Equation. *Computers and Mathematics with Applications*, **75**, 4214-4220. https://doi.org/10.1016/j.camwa.2018.03.023